Performance of Orbital Rendezvous Radar

Benjamin GIGLEUX[1, 2] François VINCENT[2] Eric CHAUMETTE[2] Thomas HUSSON[3]

[1]ONERA/DEMR, Université de Toulouse, F-31055 Toulouse, France

[2]ISAE-SUPAERO, Université de Toulouse, DEOS Dept., Toulouse, France

[3]Thalès Service, 290 Allée du Lac, 31670 Labège, France

Résumé – Un rendez-vous spatial est une manœuvre au cours de laquelle un véhicule spatial, appelé chasseur, s'approche d'une cible dans un même plan orbital. Cet article étudie le cas d'un rendez-vous en orbite circulaire, et estime la précision atteignable par un radar pour le contrôle précis du chasseur.

Abstract – A space rendezvous is a maneuver during which a spacecraft, namely the chaser, approaches a target in the same orbital plane. This paper studies the case of rendezvous in a circular orbit, and estimates the precision of a radar as support of precise control of the chaser.

1 Introduction

Space rendezvous and formation flying started in 1965 when the Gemini missions were preparing the various orbital maneuvers of the Apollo program [2]. Space rendezvous were then decisive for the implementation of the Apollo lunar missions and for the assembly and refueling of the Mir and the International Space Station (ISS). An astronaut, usually guided by lidar or radar [3] systems, controls a space vehicle (namely the chaser) to approach a cooperative target during these missions. Nowadays, in-orbit servicing and active debris removal strengthen the stake in autonomous space rendezvous [5]. The chaser will most likely host various sensors such as camera, lidar or radar to ensure the safety of operations. For that purpose, the estimation of the relative motion between the chaser and its target from discrete radar observations is studied. Circular orbits are assumed, which enables to consider the well-known Clohessy-Wiltshire (CW) motion model [4].

The paper is organized as follow: first the models describing the orbital relative motion and the radar measurements are presented. Then, the Fisher Information Matrix (FIM) is computed for the motion parameter estimation from discrete radar observations during long-range space rendezvous. Finally, a comparison with the Maximum Likelihood Estimation (MLE) is performed to assess the validity of the FIM.

The results of this paper may be used as in [6] where a similar approach is proposed. The FIM is determined for bearing-only measurements and is exploited to optimize the fuel consumption of the chaser while maintaining the observability of the target during space rendezvous.

2 Model

2.1 Orbital Relative Motion

Clohessy and Wiltshire have demonstrated that the restricted three-body problem involving the chaser (C) nearby its target (T) in a circular orbit around the Earth (E) results in a relative motion that is entirely defined from the initial relative position and speed between C and T. To describe this motion, the CW frame, $\mathcal{R} = \{C, x, y, z\}$, is introduced as the right-handed orthonormal frame with x in the direction of zenith of the point C, and y tangent to the orbit at the point C and in the direction of its motion (cf. figure 1). The coordinates of the target in $\mathcal{R}$ are taken to be $T = (x, y, z)^T$.

$$X(t) = \begin{bmatrix} F(t) \\ \dot{F}(t) \end{bmatrix} X(0), \tag{1}$$

where $X(t) = [x(t)\ y(t)\ z(t)\ \dot{x}(t)\ \dot{y}(t)\ \dot{z}(t)]^T$ is the state vector describing the relative motion, and $F(t)$ is a 3×6 matrix defined as follow: $F_{1,1}(t) = 4 - 3\cos(\omega t)$; $F_{2,1}(t) = 6(\sin(\omega t) - \omega t)$; $F_{2,2}(t) = 1$; $F_{3,3}(t) = \cos(\omega t)$; $F_{1,4}(t) = (1/\omega)\sin(\omega t)$; $F_{2,4}(t) = -(2/\omega)(1 - \cos(\omega t))$; $F_{1,5}(t) = (2/\omega)(1 - \cos(\omega t))$; $F_{2,5}(t) = (1/\omega)(4\sin(\omega t) - 3\omega t)$; $F_{3,6}(t) = (\sin(\omega t)/\omega)$; while other terms of $F(t)$ are null. Finally, ω is the angular rate and depends on the altitude.

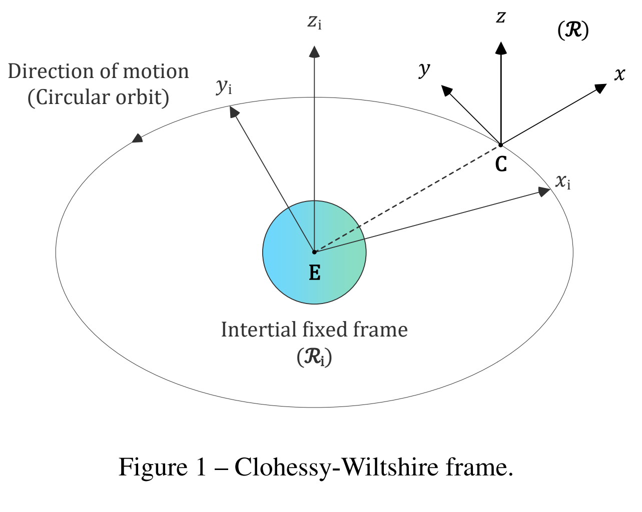

Figure 1 – Clohessy-Wiltshire frame.

2.2 Radar Observations

A radar, onboard the chaser, observes the target during the time window $[-T_o/2 \ \ +T_o/2]$ and uniformly samples the target parameters, namely θ, comprising the range (r), the range-rate ($\dot{r}$), and both direction cosines ($u_{x'}, u_{z'}$) within the radar frame $\mathcal{R}' = \{C, x', y', z'\}$. To estimate those parameters, the radar integrates the received signal during $T_i = T_o/S$. In general, the radar processing chain is implemented as the Maximum Likelihood Estimator (MLE) which justifies that the radar measurements asymptotically follow a Gaussian distribution at high Signal-to-Noise Ratio (SNR):

$$\hat{\theta}(t_s) = \left[\hat{r}(t_s)\; \hat{\dot{r}}(t_s)\; \hat{u}_{x'}(t_s)\; \hat{u}_{z'}(t_s)\right]^T \sim \mathcal{N}\left(0, J^{-1}(t_s)\right),$$

where $J(t_s)$ the FIM about the target parameter $\theta(t_s)$ sampled around $t_s = (s - S/2)T_i$ for $s = 1, 2, \ldots, S$. In this paper, $J(t_s)$ is supposed to be diagonal (i.e. no coupling) to simplify the calculation. Finally, the transformation matrix between the radar frame ($\mathcal{R}'$) and the CW frame ($\mathcal{R}$) is defined as $[x(t)\; y(t)\; z(t)]^T = Q(t)[x'(t)\; y'(t)\; z'(t)]^T$ where x', y' and z' relate to the target parameters:

$$\begin{bmatrix} r \\ \dot{r} \\ u_{x\prime} \\ u_{y\prime} \end{bmatrix} = \frac{1}{\sqrt{x'^2 + y'^2 + z'^2}} \begin{bmatrix} x'^2 & + y'^2 & + z'^2 \\ x'\dot{x}' & + y'\dot{y}' & + z'\dot{z}' \\ x' & & \\ & & z' \end{bmatrix}$$

3 Estimation of the Relative Motion from Radar Observations

The problem consists in estimating the initial state vector, $X_0 = X(0)$, which defines the complete target motion in the CW coordinates system, from discrete radar observations. To simplify the problem, the center of the radar receiver is assumed to coincide with the chaser center of mass. This implies that the lever arm correction is not necessary. In addition, the angular rate, ω, is assumed to be known. Moreover, the radar observations are supposed to be uniformly acquired in a short period of time with respect to the angular rate, such that the variations of the state vector $X(t)$ are limited. This assumption enables to consider the target as non-fluctuating (Swerling 0) and the distribution of scattering points can thereby be neglected in the error budget (therefore: $\forall s, J[s] \simeq J$). Finally, during space rendezvous, the off-track components, namely $x(t)$ and $z(t)$, are assumed to be maintained as a fraction of the along-track component, namely $y(t)$.

The FIM for the estimation of the parameter vector $X(0)$ from discrete radar observations is now computed. Slepian and Bangs have established the expression of the FIM in the case of real Gaussian signals [1]. Applying this result to S independent radar scans gives the FIM for the estimation of the parameter vector $X(0)$:

$$I_{p,q} = \frac{1}{2}\,\mathrm{Tr}\left\{\boldsymbol{J}^{-1}\frac{\partial \boldsymbol{J}}{\partial (X_0)_p}\boldsymbol{J}^{-1}\frac{\partial \boldsymbol{J}}{\partial (X_0)_q}\right\} + \frac{\partial\theta^H\left[\{1,2,\ldots,S\}, X_0\right]}{\partial (X_0)_p}\,\boldsymbol{J}\,\frac{\partial\,\theta\left[\{1,2,\ldots,S\}, X_0\right]}{\partial (X_0)_q},$$

where $\boldsymbol{J} = \mathrm{diag}\{J(t_1), J(t_2), \ldots, J(t_S)]\}$ is a block diagonal matrix whose blocks are the FIM of individual radar scans. Developing the calculation produces:

$$I_{p,q} = I^{r}_{p,q} + I^{\dot{r}}_{p,q} + I^{u_{x'}}_{p,q} + I^{u_{z'}}_{p,q}, \qquad (2)$$

where $I^{r}_{p,q}$ accounts for the information provided by the range, $I^{\dot{r}}_{p,q}$ by the range-rate, $I^{u_{x'}}_{p,q}$ and $I^{u_{z'}}_{p,q}$ by the direction-cosines. The contribution of each term is detailed below and the overall error budget is discussed afterwards to give an insight into a radar architecture and maneuvering strategy to perform space rendezvous.

3.1 Contribution of the Range

The contribution of the range equals:

$$I^{r}_{p,q} \triangleq \sum_{s=1}^{S}\frac{\partial\, r(t_s, X_0)}{\partial\,(X_0)_p}\,J_{1,1}(t_s)\,\frac{\partial\, r(t_s, X_0)}{\partial\,(X_0)_q}.$$

Acknowledging that the range varies little over the integration time, the contribution of the range can be approximated as:

$$I^{r}_{p,q} \simeq \frac{J_{1,1}}{r^2(0, X_0)} \times (F(0)\;X_0)^T\,\frac{1}{T_i}\int_{-\frac{T_o}{2}}^{+\frac{T_o}{2}} FF_{p,q}(t)dt\;(F(0)\;X_0),$$

with:

$$FF_{p,q}(t) = \begin{bmatrix} F_{1,p}(t) \\ F_{2,p}(t) \\ F_{3,p}(t) \end{bmatrix}\left[F_{1,q}(t)\;F_{2,q}(t)\;F_{3,q}(t)\right].$$

3.2 Contribution of the Range-Rate

The contribution of the range-rate is:

$$I^{\dot{r}}_{p,q} = \sum_{s=1}^{S}\frac{\partial\,\dot{r}(t_s, X_0)}{\partial\,(X_0)_p}\,J_{2,2}(t_s)\,\frac{\partial\,\dot{r}(t_s, X_0)}{\partial\,(X_0)_q}$$

Similarly to the contribution of the range, the contribution of the range-rate can be approximated as:

$$I^{\dot{r}}_{p,q} \simeq \frac{J_{2,2}}{r^2(0, X_0)} \times (\dot{F}(0)\;X_0)^T\,\frac{1}{T_i}\int_{-\frac{T_o}{2}}^{+\frac{T_o}{2}} F\dot{F}_{p,q}(t)dt\;(\dot{F}(0)\;X_0) + (F(0)\;X_0)^T\,\frac{1}{T_i}\int_{-\frac{T_o}{2}}^{+\frac{T_o}{2}} \dot{F}\dot{F}_{p,q}(t)dt\;(F(0)\;X_0),$$

with:

$$F\dot{F}_{p,q}(t) = \begin{bmatrix} \dot{F}_{1,p}(t) \\ \dot{F}_{2,p}(t) \\ \dot{F}_{3,p}(t) \end{bmatrix}\left[F_{1,q}(t)\;F_{2,q}(t)\;F_{3,q}(t)\right],$$

$$\dot{F}\dot{F}_{p,q}(t) = \begin{bmatrix} \dot{F}_{1,p}(t) \\ \dot{F}_{2,p}(t) \\ \dot{F}_{3,p}(t) \end{bmatrix}\left[\dot{F}_{1,q}(t)\;\dot{F}_{2,q}(t)\;\dot{F}_{3,q}(t)\right].$$

3.3 Contribution of the Direction-Cosines

The contributions of the direction-cosines are:

$$\begin{cases} I^{u_{x'}}_{p,q} = \sum_{s=1}^{S} \frac{\partial\, u_{x'}(t_s, X_0)}{\partial\, (X_0)_p}\, J_{3,3}(t_s)\, \frac{\partial\, u_{x'}(t_s, X_0)}{\partial\, (X_0)_q}, \\ I^{u_{z'}}_{p,q} = \sum_{s=1}^{S} \frac{\partial\, u_{z'}(t_s, X_0)}{\partial\, (X_0)_p}\, J_{4,4}(t_s)\, \frac{\partial\, u_{z'}(t_s, X_0)}{\partial\, (X_0)_q}. \end{cases}$$

Recalling that the off-track components are assumed to be maintained as a fraction of the along-track component, and assuming that the chaser is stabilized ($Q(t) \simeq Q(0)$), the contribution of the direction-cosines can be approximated as:

$$\begin{cases} I^{u_{x'}}_{p,q} \simeq \sum_{s=1}^{S} \frac{J_{3,3}}{r^2(0, X_0)} \quad [Q^{-1}_{1,1}(0) \quad 0 \quad Q^{-1}_{1,3}(0)] \times \\ \quad \frac{1}{T_i} \int_{-\frac{T_o}{2}}^{+\frac{T_o}{2}} FF_{p,q}(t) dt \quad [Q^{-1}_{1,1}(0) \quad 0 \quad Q^{-1}_{1,3}(0)]^T. \\ I^{u_{z'}}_{p,q} \simeq \sum_{s=1}^{S} \frac{J_{4,4}}{r^2(0, X_0)} \quad [Q^{-1}_{3,1}(0) \quad 0 \quad Q^{-1}_{3,3}(0)] \times \\ \quad \frac{1}{T_i} \int_{-\frac{T_o}{2}}^{+\frac{T_o}{2}} FF_{p,q}(t) dt \quad [Q^{-1}_{3,1}(0) \quad 0 \quad Q^{-1}_{3,3}(0)]^T. \end{cases}$$

3.4 Discussion

Developing the calculation results in the expression of the FIM for the estimation of the parameter vector $X(0)$ from discrete radar observations. For the sake of compacity, only its diagonal terms are detailed in table 1. Examining those terms in the case of a typical radar design shows that during space rendezvous, when the off-track components, namely $x(t)$ and $z(t)$, are assumed to be maintained as a fraction of the along-track component, namely $y(t)$:

1. Most information about x_0, is provided by the direction cosines: $I_{1,1} \simeq S/r^2\, (J_{3,3}\, (Q^{-1}_{1,1})^2 + J_{4,4}\, (Q^{-1}_{3,1})^2)$,
2. Most information about y_0, is provided by the range: $I_{2,2} \simeq S\, J_{1,1}$,
3. Most information about z_0, is provided by the direction cosines: $I_{3,3} \simeq S/r^2\, (J_{3,3}\, (Q^{-1}_{1,3})^2 + J_{4,4}\, (Q^{-1}_{3,3})^2)$,
4. Most information about $\dot{x}_0$, is provided by the range and range-rate thanks to the coupling between x, y, $\dot{x}$ and $\dot{y}$ in equation (1). The direction cosines enable to better condition the problem when only few radar scans are available: $I_{4,4} \simeq S\, (J_{1,1}\, \omega^2 {T_o}^4/80 + J_{2,2}\, \omega^2 {T_o}^2/3)$,
5. Most information about $\dot{y}_0$, is provided by the range and range-rate: $I_{5,5} \simeq S\, (J_{1,1}\, {T_o}^2/12 + J_{2,2})$,
6. Most information about $\dot{z}_0$, is provided by the direction cosines: $I_{6,6} \simeq S/r^2\, {T_o}^2/12\, (J_{3,3}\, (Q^{-1}_{1,3})^2 + J_{4,4}\, (Q^{-1}_{3,3})^2)$.

Those observations show that a careful attention should be given to the interpolation of range and range-rate to maximize the information about y_0, $\dot{x}_0$ and $\dot{y}_0$. In addition, the relative motion between the target and the chaser is not sufficient to exploit a synthetic antenna for the estimation of x_0, z_0 and $\dot{z}_0$. This advocates for the use of a larger antenna array along the z axis to improve the measurement of $\dot{z}_0$. Eventually, the radar should be orientated perpendicular to the orbit of the chaser (i.e. $Q(t) = Id$) to maximize the information provided by the direction cosines on the initial position and speed in the perpendicular plane to the chaser orbit.

4 Numerical Application

A space rendezvous with a non-fluctuating target is considered. The chaser realizes a thrust maneuver with an impulsive change in velocity to initiate the rendezvous. After the maneuver, the radar estimates the initial state vector resulting from the thrust. The transformation matrix $Q(t)$ is set at the identity matrix while the initial state vector is (in MKSI): $X_0 = [0 \ \ 5000 \ \ 0 \ \ 1 \ \ 0 \ \ 0]^T$. The radar observes the signal up to $T_o = 100$ seconds with a scanning rate of 1 Hz (i.e. $T_i = 1$ second). The FIM about the target parameters is simulated through a radar link budget and is almost constant as supposed in section 3. The diagonal terms of the FIM are detailed in table 2. Eventually, the Mean Squared Errors (MSE) for both the position and speed estimated by the linearized Maximum Likelyhood Estimator (MLE) are computed using Monte-Carlo simulations (100 runs) and compared to the Cramer-Rao Bound (CRB) derived from the FIM in equation (2). The linearized MLE asymptotically converges to the CRB in figures 2 and 3 as expected which verifies the proposed FIM. Besides, it can be observed that the estimates are more precise along the y dimension as the range and Doppler almost result from the respective projections of the position and speed on this axis. In addition, the speed estimate along the x dimension benefits from the coupling between $\dot{x}$ and $\dot{y}$ in equation (1), which explains why it becomes more precise than the speed estimate along the z dimension. The lattest is indeed independent from both other dimensions. Finally, the position estimates along both x and z dimensions have similar precision as they mostly result from the direction cosines which have the same precision in this numerical application.

Table 2 – Standard deviations for the radar observations.

Range error: $(J_{1,1})^{-1/2} = 5.3 \times 10^{-2}\ [m]$
Range-rate error: $(J_{2,2})^{-1/2} = 1.6 \times 10^{-4}\ [m.s^{-1}]$
Direction cosine errors for the unit vectors x/r and z/r: $(J_{3,3})^{-1/2} = (J_{4,4})^{-1/2} = 4.7 \times 10^{-4}$

5 Conclusion

The FIM for the estimation of the orbital relative motion from discrete radar observations has been established in the case of rendezvous in circular orbits. The FIM can be used to design a space-based radar with respect to the specified performances; or can be computed onboard the radar to decide when enough measurements have been collected to estimate the relative position between the chaser and its target during rendezvous and proximity operations. Nonetheless, one shall

Table 1 – Diagonal terms of the FIM for the estimation of the X_0 from discrete radar observation

$$I_{1,1} = \frac{S}{r^2}\Bigg\{\left(J_{1,1} + J_{2,2}\,\frac{3\,\omega^4 {T_o}^2}{4}\right) x^2(0) + \left(J_{1,1}\,\frac{\omega^6 {T_o}^6}{448} + J_{2,2}\,\frac{9\,\omega^6 {T_o}^4}{80}\right) y^2(0) + \left(J_{2,2}\right) \dot{x}^2(0) + \left(J_{2,2}\,\frac{\omega^6 {T_o}^6}{448}\right) \dot{y}^2(0) + \left(J_{3,3}\,(Q^{-1}_{1,1})^2 + J_{4,4}\,(Q^{-1}_{3,1})^2\right)\Bigg\}$$

$$I_{2,2} = \frac{S}{r^2}\Big\{J_{1,1}\; y^2(0) + J_{2,2}\; \dot{y}^2(0)\Big\}$$

$$I_{3,3} = \frac{S}{r^2}\Bigg\{\left(J_{1,1} + J_{2,2}\,\frac{\omega^4 {T_o}^2}{12}\right) z^2(0) + \left(J_{2,2}\right) \dot{z}^2(0) + \left(J_{3,3}\,(Q^{-1}_{1,3})^2 + J_{4,4}\,(Q^{-1}_{3,3})^2\right)\Bigg\}$$

$$I_{4,4} = \frac{S}{r^2}\Bigg\{\left(J_{1,1}\,\frac{{T_o}^2}{12} + J_{2,2}\right) x^2(0) + \left(J_{1,1}\,\frac{\omega^2 {T_o}^4}{80} + J_{2,2}\,\frac{\omega^2 {T_o}^2}{3}\right) y^2(0) + \left(J_{2,2}\,\frac{{T_o}^2}{12}\right) \dot{x}^2(0) + \left(J_{2,2}\,\frac{\omega^2 {T_o}^4}{80}\right) \dot{y}^2(0) + \left(J_{3,3}\,\frac{{T_o}^2}{12}\,(Q^{-1}_{1,1})^2 + J_{4,4}\,\frac{{T_o}^2}{12}\,(Q^{-1}_{3,1})^2\right)\Bigg\}$$

$$I_{5,5} = \frac{S}{r^2}\Bigg\{\left(J_{1,1}\,\frac{\omega^2 {T_o}^4}{80} + J_{2,2}\,\frac{\omega^2 {T_o}^2}{3}\right) x^2(0) + \left(J_{1,1}\,\frac{{T_o}^2}{12} + J_{2,2}\right) y^2(0) + \left(J_{2,2}\,\frac{\omega^2 {T_o}^4}{80}\right) \dot{x}^2(0) + \left(J_{2,2}\,\frac{{T_o}^2}{12}\right) \dot{y}^2(0)\Bigg\}$$

$$I_{6,6} = \frac{S}{r^2}\Bigg\{\left(J_{1,1}\,\frac{{T_o}^2}{12} + J_{2,2}\right) z^2(0) + \left(J_{2,2}\,\frac{{T_o}^2}{12}\right) \dot{z}^2(0) + \left(J_{3,3}\,\frac{{T_o}^2}{12}\,(Q^{-1}_{1,3})^2 + J_{4,4}\,\frac{{T_o}^2}{12}\,(Q^{-1}_{3,3})^2\right)\Bigg\}$$

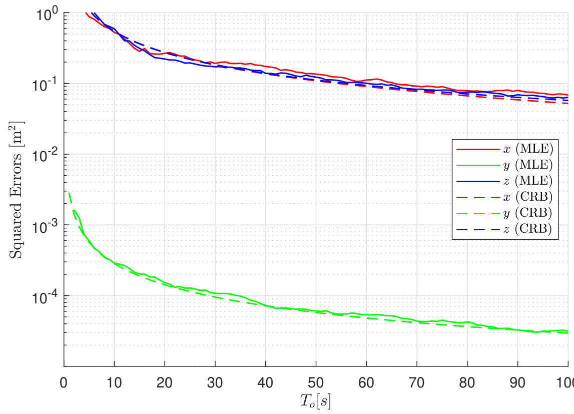

Figure 2 – Position Errors.

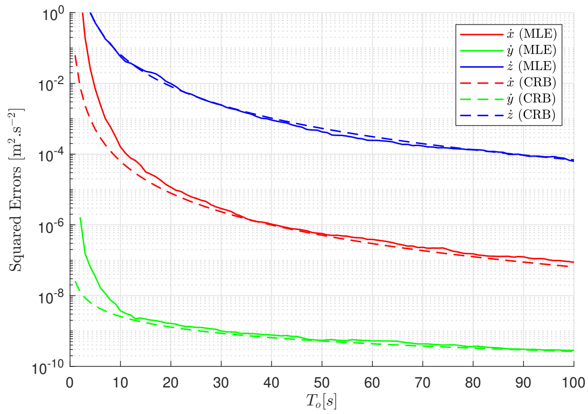

Figure 3 – Speed Errors.

keep in mind that the target is in practice not a single scattering point and that the distribution of scattering points is expected to impact the error budget.

References

[1] William John Bangs. *Array Processing with Generalized Beam-Formers*. PhD thesis, Yale University, 1971.

[2] Aldrin Buzz. *Line-of-sight Guidance Techniques for Manned Orbital Rendezvous*. PhD thesis, Massachusetts Institute of Technology, 1963.

[3] Leopold J. Cantafio. *Space-Based Radar Handbook*. Archtech House, Boston, USA, 1989.

[4] W. H. Clohessy and R. S. Wiltshire. Terminal guidance system for satellite rendezvous. *Journal of the Aerospace Sciences*, 27(9):653–658, 1960.

[5] David Charles Woffinden. *Angles-Only Navigation for Autonomous Orbital Rendezvous*. PhD thesis, Utah State University, 2008.

[6] Chu Xiaoyu, Liang Zongchuang, and Li Yanyan. Trajectory optimization for rendezvous with bearing-only tracking. *Acta Astronautica*, 171:311–322, 2020.